Electronic Supplementary Material (ESI) for Journal of Materials Chemistry A.

Supporting information

for

Strain induced rich planar defects in heterogeneous WS_2/WO_2 enable efficient nitrogen fixation at low overpotential

Ying Ling[a#], Farhad MD Kazim[a#], Shuangxiu Ma[a#], Quan Zhang[a], Konggang Qu[b], Yangang Wang[c*], Shenglin Xiao[a], Weiwei Cai[a*] and Zehui Yang[a*]

[a]Sustainable Energy Laboratory, Faculty of Materials Science and Chemistry, China University of Geosciences, Wuhan, 430074, China.

[b]Shandong Provincial Key Laboratory/Collaborative Innovation Center of Chemical Energy Storage & Novel Cell Technology, Liaocheng University, Liaocheng, 252059, China.

[c]College of Biological Chemical Science and Engineering, Jiaxing University, Jiaxing 314001, China.

#Y. Ling, F. Kazim and S. Ma equally contributed to this work.

*Corresponding authors: ygwang8136@mail.zjxu.edu.cn (Y. Wang); willcai1985@gmail.com (W. Cai); yeungzehui@gmail.com (Z. Yang)

Table S1. Summary of electrochemical NRR performance at different potential and electrolyte.

Catalyst	Electrolyte	NH_3 yield rate ($\mu g\ h^{-1}\ mg^{-1}$)	FE (%)	Applied potential	Reference
WS_2/WO_2	0.05 M H_2SO_4	8.53	13.5	-0.1 V vs RHE	this work
Mo_2C/C	0.5M Li_2SO_4	11.3	7.8	-0.3 V vs RHE	S1
Mo-SACs	0.1 M KOH	30.4	13	-0.3 V vs RHE	S2
PCN	0.1 M HCl	8.09	11.59	-0.2 V vs RHE	S3
Bi_4V_2O11/CeO_2	0.1 M HCl	23.21	10.16	-0.2 V vs RHE	S4
Pd/C	0.1 M PBS	4.5	8.2	0.1 V vs RHE	S5
Au nanorod	0.1 M KOH	1.65	3.88	-0.2 V vs RHE	S6
Au cluster/TiO_2	0.1 M HCl	21.4	8.11	-0.2 V vs RHE	S7
α-Au/CeOx-RGO	0.1 M HCl	8.3	10.1	-0.2 V vs RHE	S8

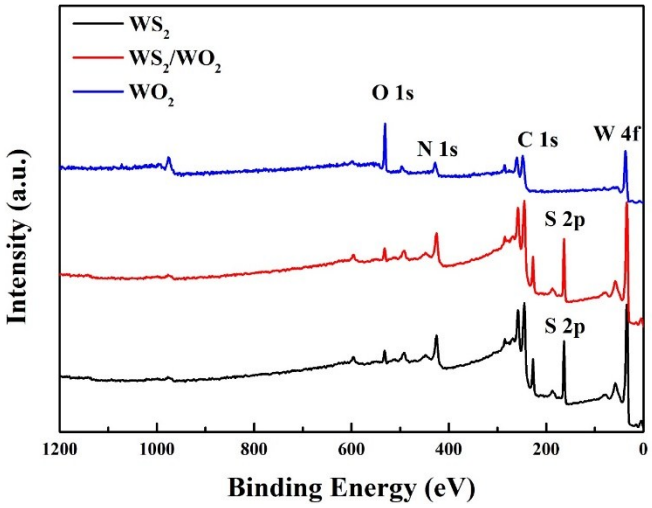

Figure S1 XPS survey scan spectra of WS_2, WS_2/WO_2 and WO_2.

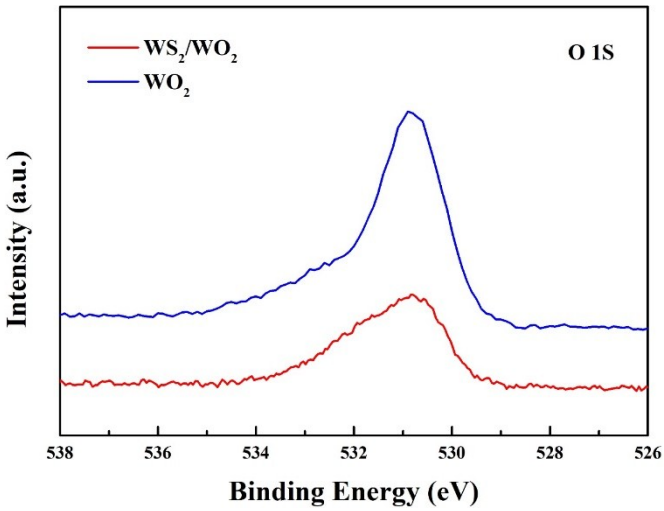

Figure S2 High-resolution O1s XPS spectra of WS_2/WO_2 and WO_2.

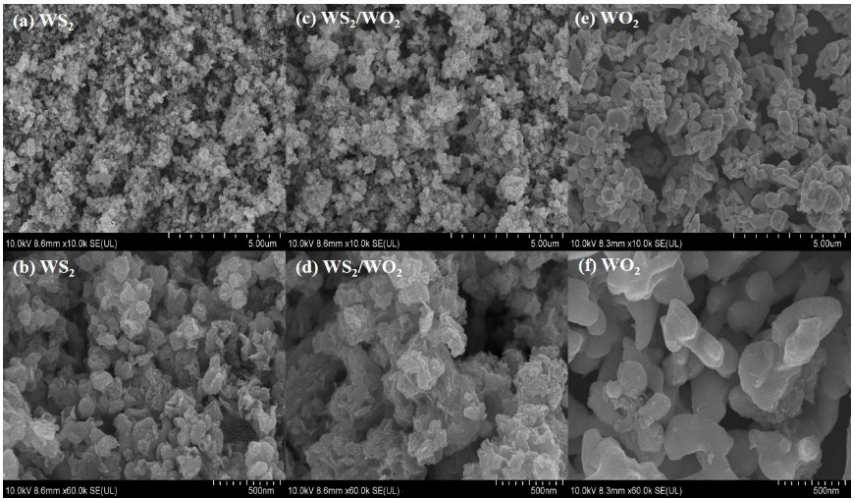

Figure S3 SEM images ofWS_2 (a, b), WS_2/WO_2 (c, d) and WO_2 (e, f).

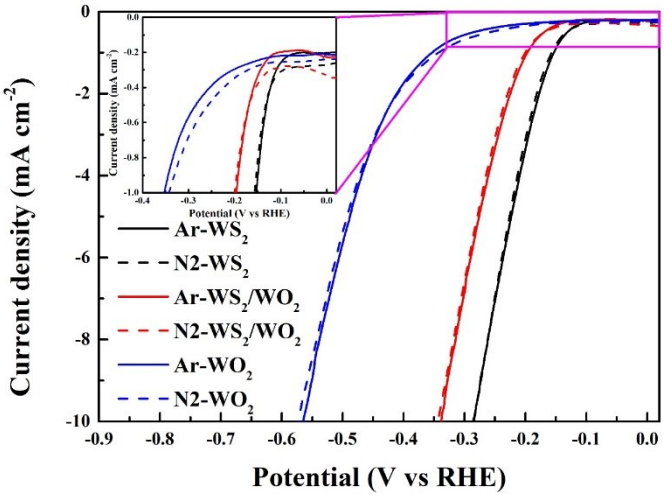

Figure S4 LSV curves of WS_2, WS_2/WO_2 and WO_2 in N_2/Ar-saturated electrolyte.

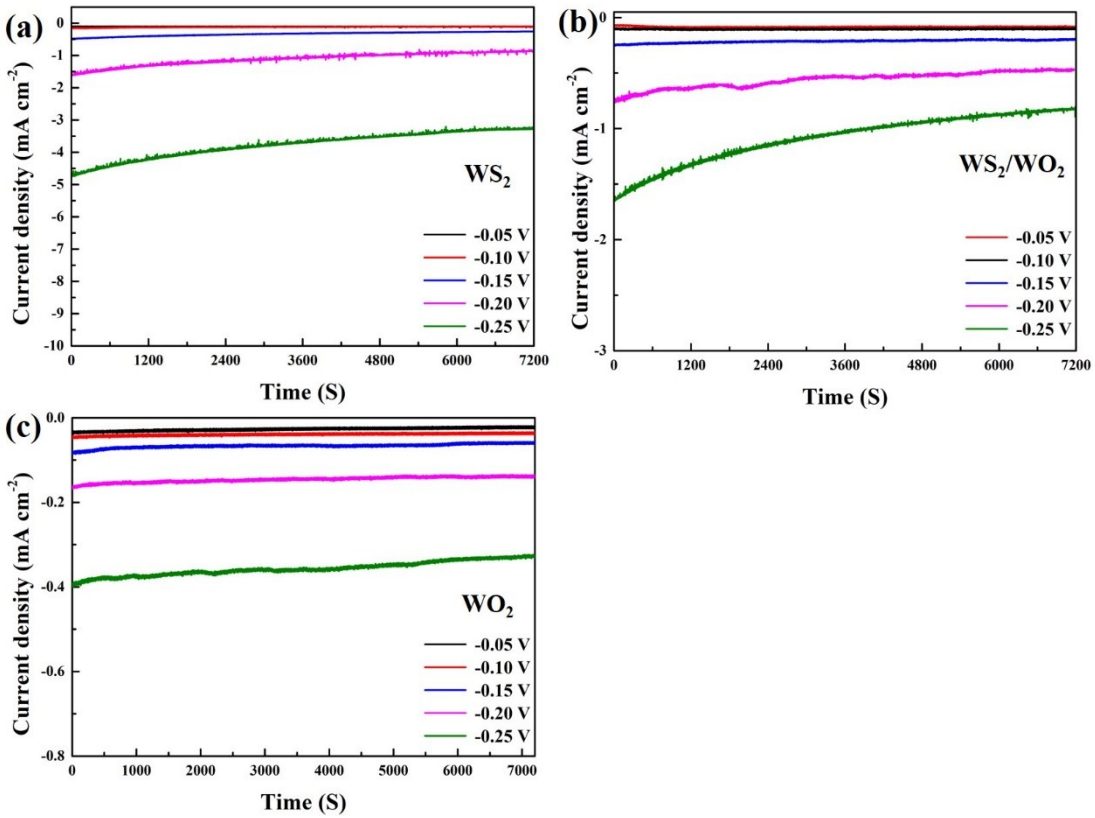

Figure S5 CA curves of WS_2 (a), WS_2/WO_2 (b) and WO_2 (c) at different potentials.

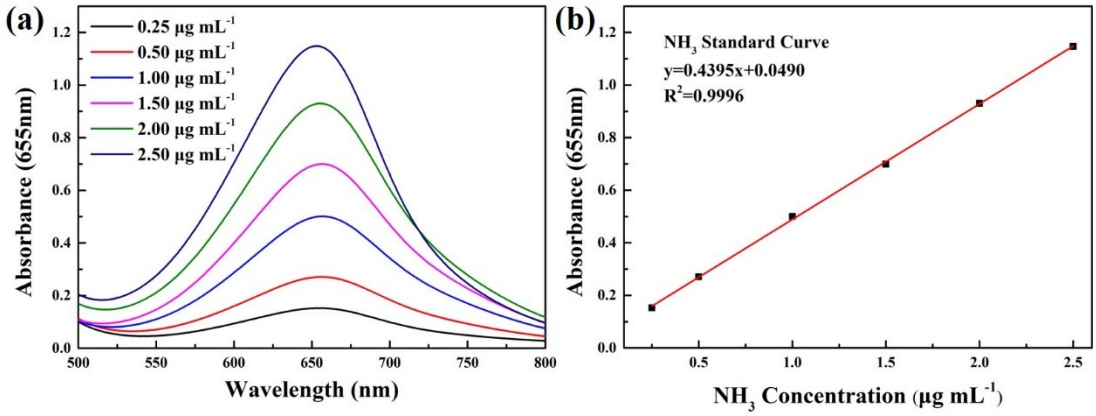

Figure S6 (a) UV-vis absorption spectra at various ammonia concentrations and (b) the corresponding NH_3 standard curve.

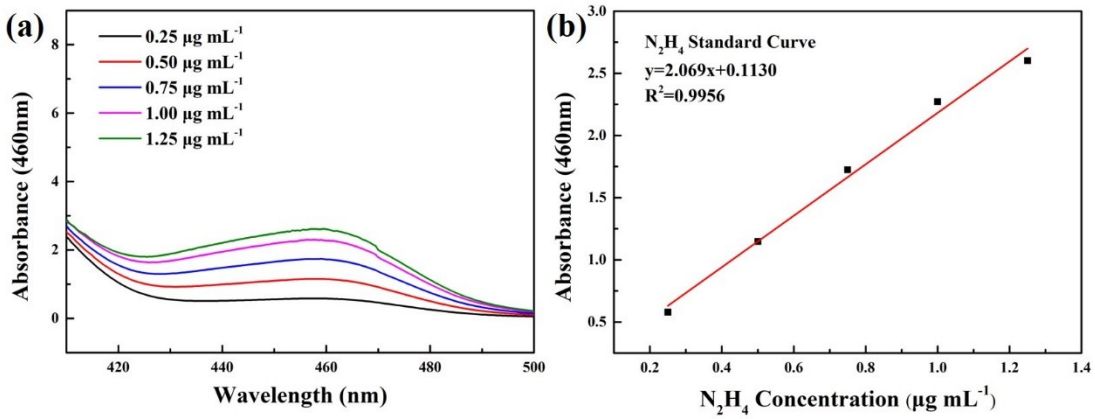

Figure S7 (a) UV-vis absorption spectra at various hydrazine concentrations and (b) the corresponding N_2H_4 standard curve.

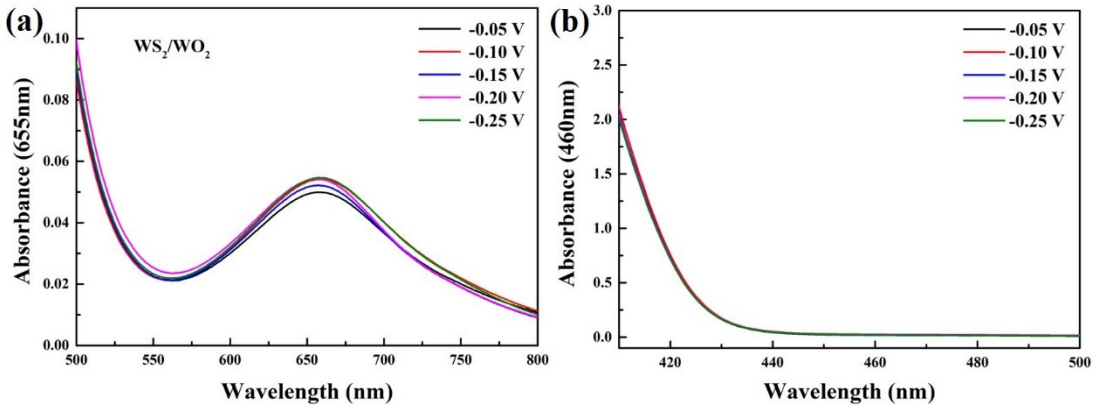

Figure S8 UV-vis absorption spectra of (a) NH_3 and (b) N_2H_4 for WS_2/WO_2 at different potentials.

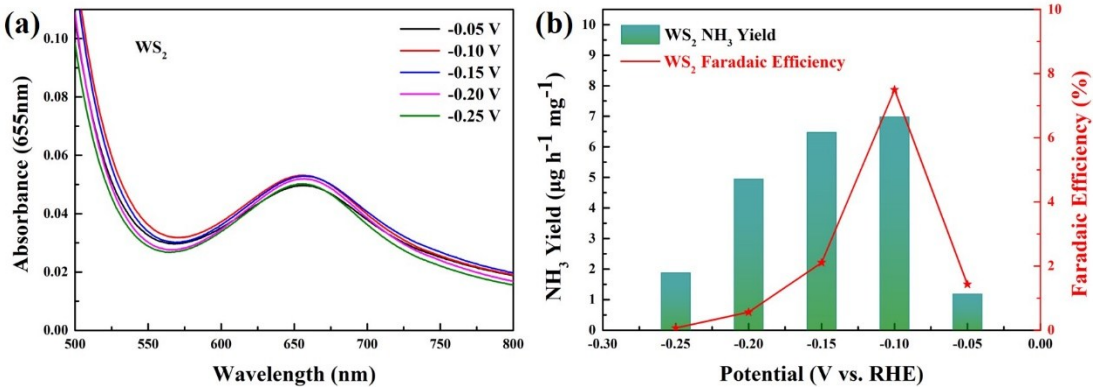

Figure S9 (a) UV-vis absorption spectra of WS_2 at different potentials and (b) NH_3 yield and Faradaic Efficiency of WS_2.

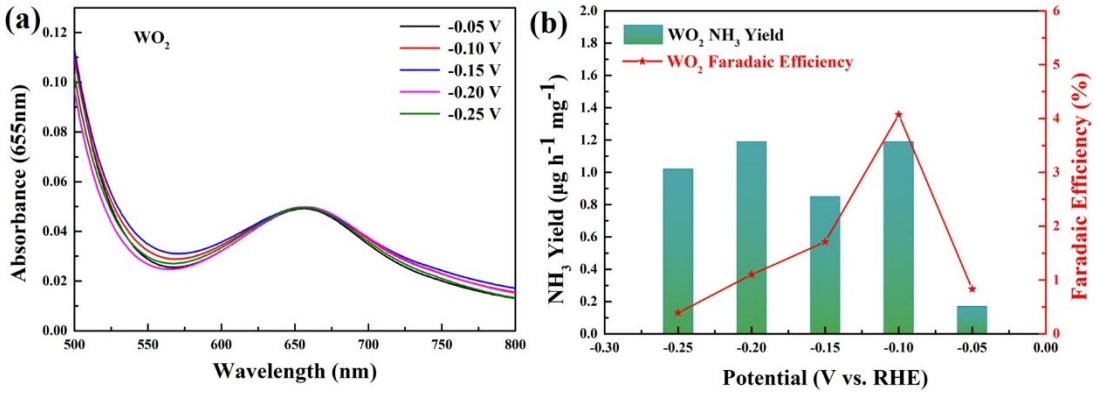

Figure S10 (a) UV-vis absorption spectra of WO_2 at different potentials and (b) NH_3 yield and Faradaic Efficiency of WO_2.

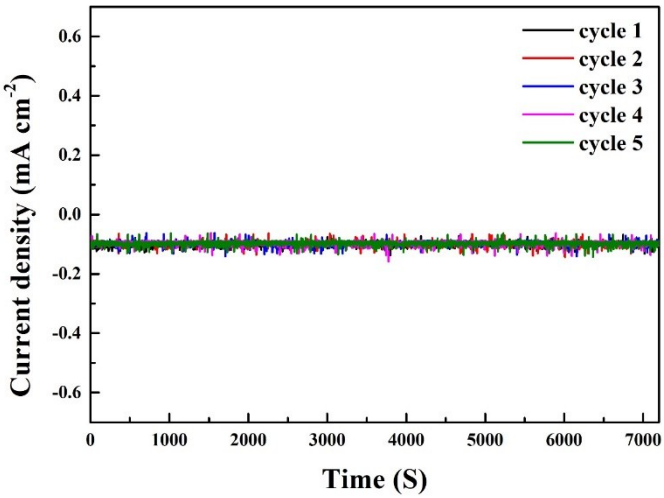

Figure S11 CA curves of WS_2/WO_2 at -0.1 V vs RHE for 5 times.

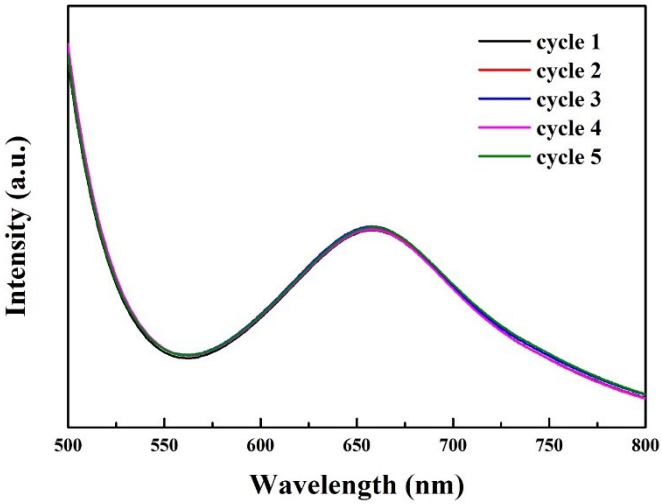

Figure S12 UV-vis absorption spectra WS_2/WO_2 at -0.1 V vs RHE for 5 times.

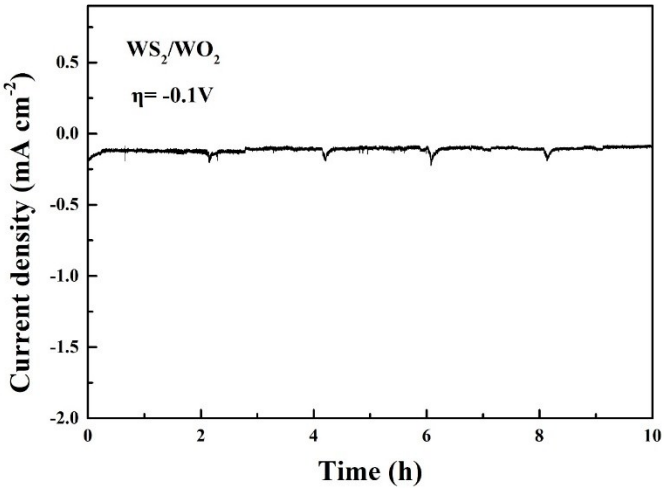

Figure S13 CA curves of WS_2/WO_2 at -0.1 V vs RHE for 10 h.

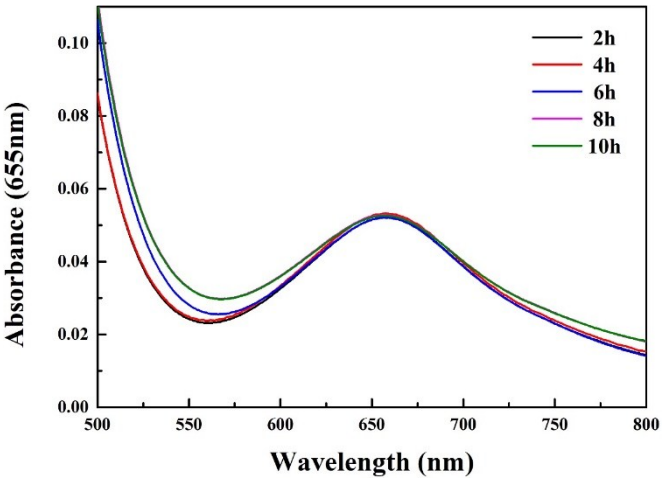

Figure S14 UV-vis absorption spectra of WS_2/WO_2 at -0.1 V vs RHE for every 2 h.

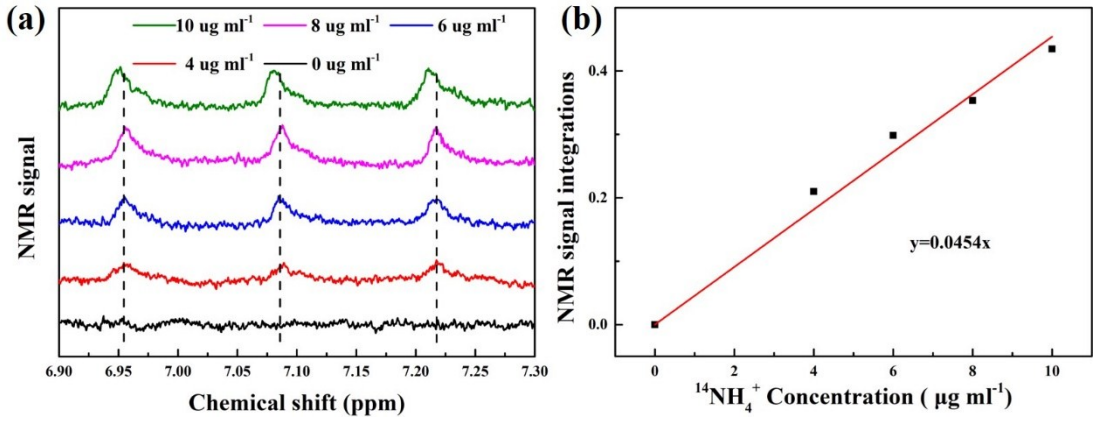

Figure S15 (a) ^{1}H NMR spectra for the $^{14}NH_4^+$ standard samples and (b) the corresponding calibration.

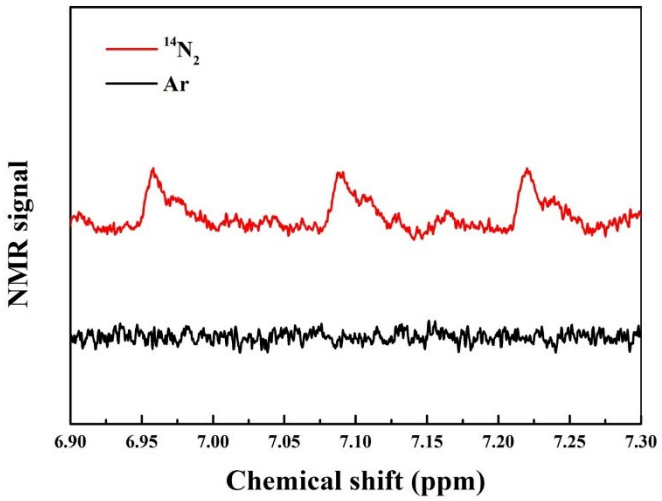

Figure S16 ^{1}H NMR spectra for the $^{14}NH_4^+$ tested in N_2- and Ar- saturated electrolyte.

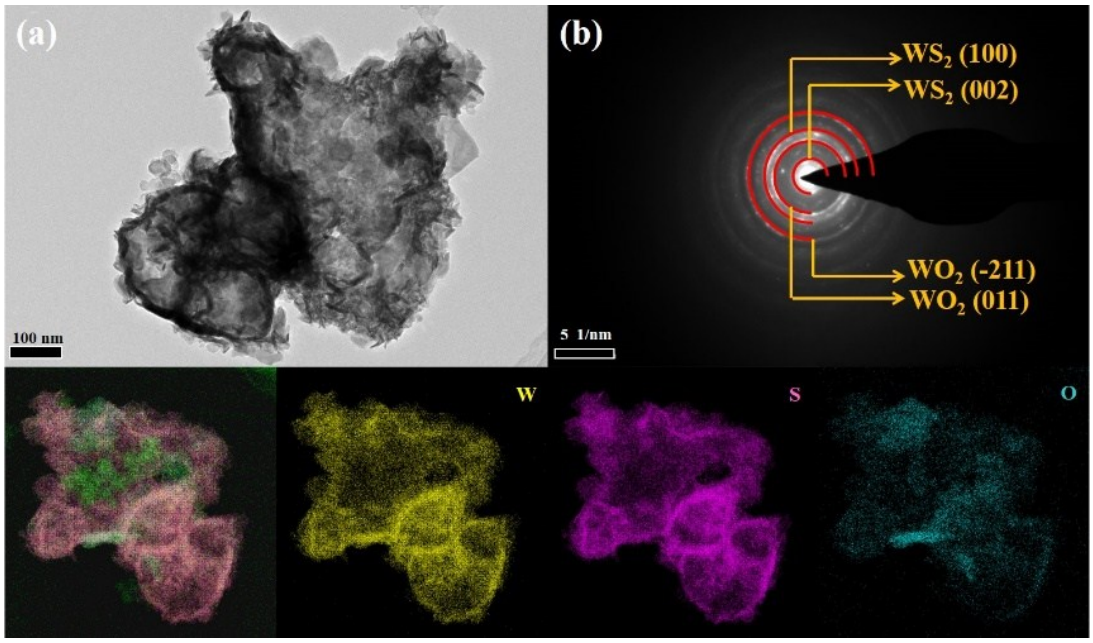

Figure S17 (a) The morphology and (b) electron diffraction and mapping of WS_2/WO_2 after 10 h catalysis.

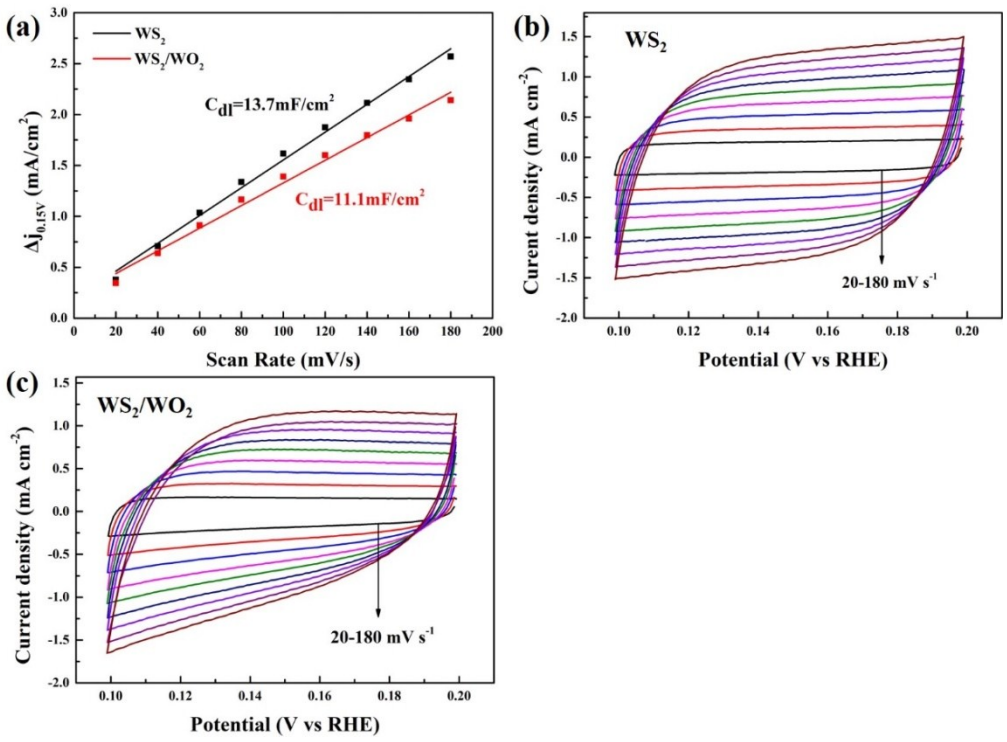

Figure S18 C_{dl} of WS_2/WO_2 and WS_2. CV curves at different scan rates of (b) WS_2/WO_2 and (c) WS_2.

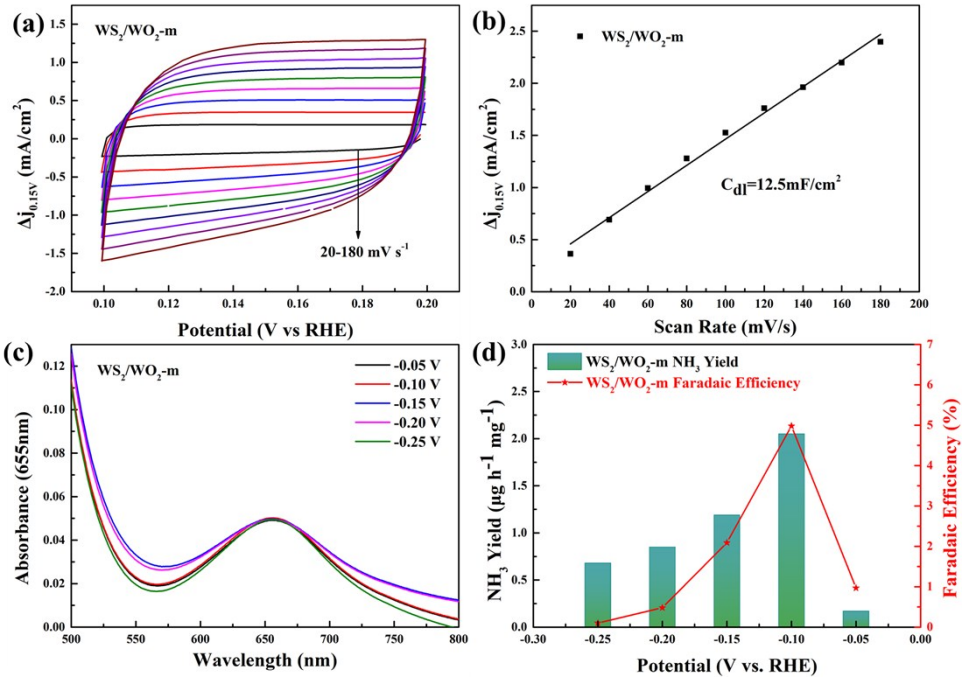

Figure S19 CV curves (a) at different scan rates and C_{dl} (b) of WS_2/WO_2-*m*. (c) UV-vis absorption spectra of WS_2/WO_2-*m* at different potentials. (d) NH_3 yield and Faradaic Efficiency of WS_2/WO_2-*m*.

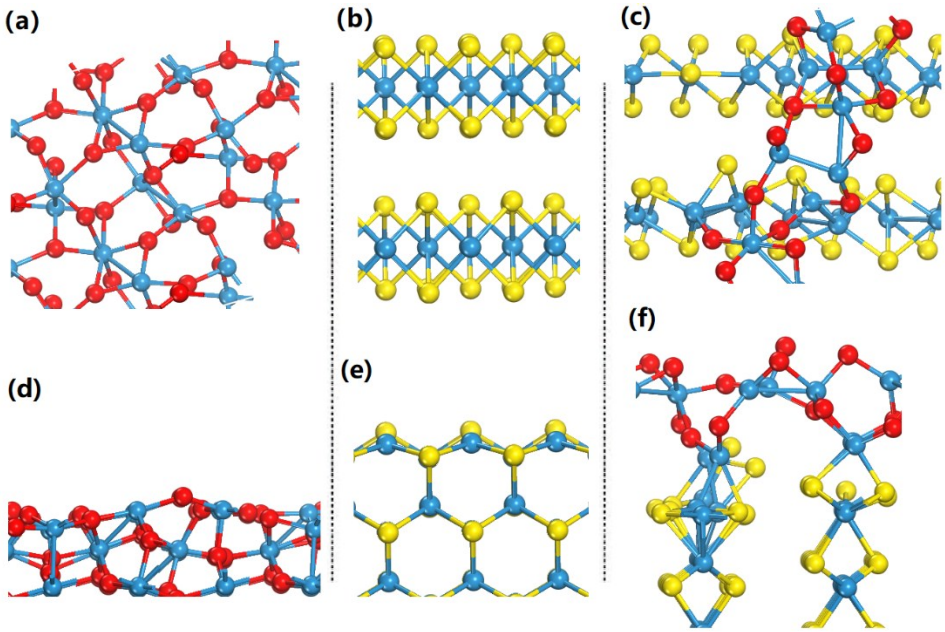

Figure S20 The top and side views of WO_2 (a, b), WS_2 (c, d) and WS_2/WO_2 (e, f) heterostructures.

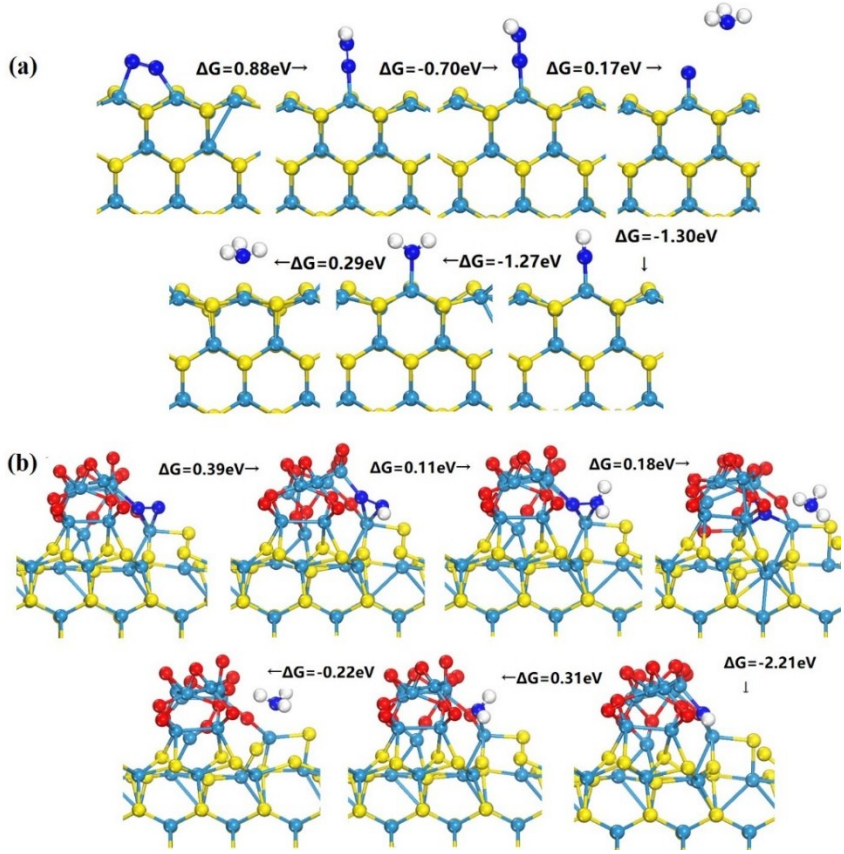

Figure S21 Reaction pathway and the corresponding energy changes for NRR of (a) WS_2 and (b) WS_2/WO_2.

References

[S1] H. Cheng, L.-X. Ding, G.-F. Chen, L. Zhang, J. Xue, H. Wang, *Adv. Mater.* **2018**, e1803694.

[S2] L. Han, X. Liu, J. Chen, R. Lin, H. Liu, F. Lu, S. Bak, Z. Liang, S. Zhao, E. Stavitski, J. Luo, R. R. Adzic, H. L. Xin, *Angew. Chem. Int. Ed.* **2019**, *58*, 2321-2325.

[S3] C. Lv, Y. Qian, C. Yan, Y. Ding, Y. Liu, G. Chen, G. Yu, *Angew. Chem. Int. Ed.* **2018**, *57*, 10246-10250.

[S4] C. Lv, C. Yan, G. Chen, Y. Ding, J. Sun, Y. Zhou, G. Yu, *Angew. Chem. Int. Ed.* **2018**, *57*, 6073-6076.

[S5] J. Wang, L. Yu, L. Hu, G. Chen, H. Xin, X. Feng, *Nat. Commun.* **2018**, *9*, 1795.

[S6] D. Bao, Q. Zhang, F. L. Meng, H. X. Zhong, M. M. Shi, Y. Zhang, J. M. Yan, Q. Jiang, X. B. Zhang, *Adv. Mater.* **2017**, *29,* 1604799.

[S7] M. M. Shi, D. Bao, B. R. Wulan, Y. H. Li, Y. F. Zhang, J. M. Yan, Q. Jiang, *Adv. Mater.* **2017**, *29*, 201606550.

[S8] S. J. Li, D. Bao, M. M. Shi, B. R. Wulan, J. M. Yan, Q. Jiang, *Adv. Mater.* **2017**, *29*, 201700001.